Supra-Canonical $^{26}Al/^{27}Al$ and the Residence Time of CAIs in the Solar Protoplanetary Disk

Edward D. Young,[1,2]* Justin I. Simon,[2] Albert Galy,[3] Sara S. Russell,[4] Eric Tonui,[2] Oscar Lovera[2]

The canonical initial $^{26}Al/^{27}Al$ ratio of 4.5×10^{-5} has been a fiducial marker for the beginning of the solar system. Laser ablation and whole-rock multiple-collector inductively coupled plasma-source mass spectrometry magnesium isotope analyses of calcium- and aluminum-rich inclusions (CAIs) from CV3 meteorites demonstrate that some CAIs had initial $^{26}Al/^{27}Al$ values at least 25% greater than canonical and that the canonical initial $^{26}Al/^{27}Al$ cannot mark the beginning of solar system formation. Using rates of Mg diffusion in minerals, we find that the canonical initial $^{26}Al/^{27}Al$ is instead the culmination of thousands of brief high-temperature events incurred by CAIs during a 10^5-year residence time in the solar protoplanetary disk.

The short-lived radionuclide ^{26}Al [mean life = 1.05 million years (My)] was an important source of heat in the early solar system (*1*). It is also a high-resolution chronometer for early solar system evolution (*2*). Its former presence in the solar system is evidenced by excesses in its decay product, $^{26}Mg^*$, correlated with Al/Mg in the constituents of meteorites (*3*). The largest excesses occur in the CAIs found in many chondrites. The CAIs are the oldest known solid objects that formed in the solar system and have absolute ^{207}Pb-^{206}Pb ages of 4567.2 ± 0.6 My (*4*). Here, we present new ultraviolet (UV) laser ablation and acid digestion multiple-collector inductively coupled plasma-source mass spectrometry (MC-ICPMS) analyses of CAIs showing that there was more ^{26}Al in the early solar system than previously thought and that the canonical $^{26}Al/^{27}Al$ is a reflection of the residence time of CAIs in the protoplanetary disk.

The use of ^{26}Al as a chronometer relies on variations in the initial $^{26}Al/^{27}Al$ ratio [$(^{26}Al/^{27}Al)_o$] in objects formed within several mean lives of ^{26}Al decay. Values for $(^{26}Al/^{27}Al)_o$ are defined by isochrons comprising linear correlations between $^{26}Mg^*/^{24}Mg$ and $^{27}Al/^{24}Mg$. The slopes of these correlations are numerically equivalent to $(^{26}Al/^{27}Al)_o$ because all of the ^{26}Al decayed away billions of years ago. Age differences are reflected in differences in $(^{26}Al/^{27}Al)_o$ if $^{26}Al/^{27}Al$ was uniform in the early solar system.

A central assumption is that the canonical $(^{26}Al/^{27}Al)_o$ value equates with an absolute age of about 4567 My and represents the initial abundance of ^{26}Al for the solar system as a whole. Most data have come from measurements of Al-rich minerals, especially anorthite, a Ca-rich feldspar mineral, because high $^{27}Al/^{24}Mg$ affords high-precision estimates of $^{26}Mg^*$. The canonical $(^{26}Al/^{27}Al)_o$ for the solar system based on these data is 4.5×10^{-5} (*5*, *6*). It has been thought that all reliable measurements of $(^{26}Al/^{27}Al)_o$ are 5×10^{-5} or less (*5*); past claims of $(^{26}Al/^{27}Al)_o$ values greater than 5×10^{-5} have been dismissed as spurious as a result of analytical errors (*5*).

Some, though not all (*7*), MC-ICPMS measurements of $^{26}Mg^*$ and Al/Mg in low-Al CAI minerals have suggested that the initial $(^{26}Al/^{27}Al)_o$ of the solar system may have been higher than the canonical value (*8*–*10*). These early data were viewed as too few to warrant revision of the canonical $(^{26}Al/^{27}Al)_o$. We present new laser-ablation MC-ICPMS Mg isotope data for six igneous CAIs from the Allende (M5, USNM 3576-1), Efremovka (E44), Grosnaja (63624-1), and Leoville (144A, MRS3) CV3 meteorites and two "fluffy" type A CAIs from the Vigarano CV3 meteorite (Vigarano 10 and Vigarano 9) (*11*). In addition, we present analyses of dissolved fragments representing substantial parts of three of the objects (Allende 3576-1, Grosnaja 63624-1, and Leoville 144A) to provide estimates of their bulk Mg isotopic compositions.

Supra-canonical $^{26}Al/^{27}Al$. Of the 284 laser-ablation analyses of the eight CAIs (table S1), most (79%) lie above the canonical line corresponding to $(^{26}Al/^{27}Al)_o = 4.5 \times 10^{-5}$ (Fig. 1). The $\delta^{26}Mg^*$ [the per mil (‰) excess in $^{26}Mg/^{24}Mg$ due to the presence of $^{26}Mg^*$] and $^{27}Al/^{24}Mg$ values are correlated, and the data for six of the eight objects are consistent with a zero intercept; the laser ablation data include isochrons corresponding to $(^{26}Al/^{27}Al)_o$ values greater than canonical. The three bulk (whole-rock) CAI values for Allende 3576-1, Grosnaja 63624-1, and Leoville 144A agree with the laser-ablation data for these objects; whole-rock and laser-ablation $\delta^{25}Mg'$ and $\delta^{26}Mg'$ values ($^{25}Mg/^{24}Mg$ and $^{26}Mg/^{24}Mg$ ex-

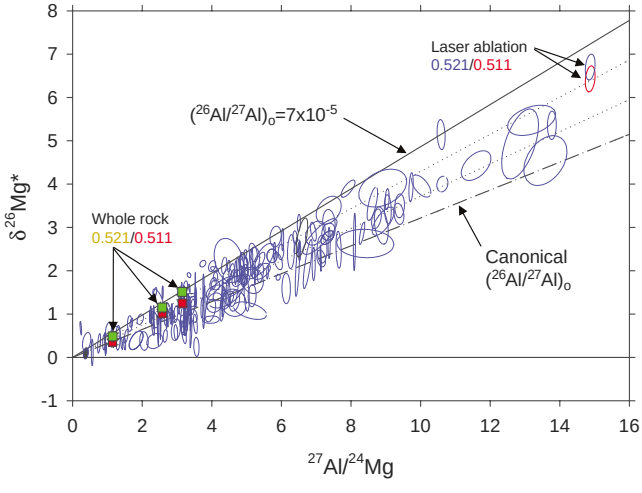

Fig. 1. Compilation of 203 analyses obtained by laser-ablation MC-ICPMS representing seven of the eight CAIs in this study (another 81 analyses of Grosnaja 63624-1 are omitted for clarity). Each datum is shown as a 1σ error ellipse. 79% of analyses are above the canonical $(^{26}Al/^{27}Al)_o$ line. $\delta^{26}Mg^*$ correlates with $^{27}Al/^{24}Mg$, and many data (e.g., 144A, Fig. 2) are consistent with a zero intercept, all of which are requisites for interpreting the results as indicative of decay of ^{26}Al with $(^{26}Al/^{27}Al)_o > 4.5 \times 10^{-5}$. Also shown are the three whole-rock CAI values represented by green squares (error bars are smaller than symbols). Red squares and the single red ellipse show the effects of recalculating the whole-rock data and the laser-ablation analyses, respectively, with a mass fractionation relationship between $\delta^{25}Mg'$ and $\delta^{26}Mg'$ of 0.511 rather than 0.521. The $(^{26}Al/^{27}Al)_o$ values of the lines in descending order from top are 7×10^{-5} (solid), 6×10^{-5} (dot), 5.2×10^{-5} (dot), 4.5×10^{-5} (canonical, dash-dot), and 0.0 (solid).

[1]Institute of Geophysics and Planetary Physics, [2]Department of Earth and Space Sciences, University of California–Los Angeles, Los Angeles, CA 90095, USA. [3]Department of Earth Sciences, University of Cambridge, Cambridge CB2 3EQ, UK. [4]The Natural History Museum, London SW7 5BD, UK.

*To whom correspondence should be addressed. E-mail: eyoung@ess.ucla.edu

pressed as per mil differences from a standard) of the objects at comparable $^{27}Al/^{24}Mg$ are consistent (table S1). Weighted linear regression (*12*) of the whole-rock data gives a model $(^{26}Al/^{27}Al)_o$ isochron of 7.0 (±1.32 2σ) × 10^{-5}, a $\delta^{26}Mg^*$ intercept of −0.1 (±0.2 2σ), and an MSWD (mean square weighted deviation) of 0.37. Regression of the whole-rock data with a 0.511 rather than a 0.521 mass-dependent isotope fractionation relationship between $\delta^{26}Mg'$ and $\delta^{25}Mg'$ gives 6.3 (±1.3 2σ) × 10^{-5}, −0.2 (±0.2 2σ), and 0.08 for $(^{26}Al/^{27}Al)_o$, $\delta^{26}Mg^*$ intercept, and MSWD, respectively.

Data for the two most thoroughly studied CAIs, 144A, a compact type A from Leoville, and E44, a type B1 from Efremovka, are used here to illustrate the evidence for high $(^{26}Al/^{27}Al)_o$ values as defined by intra-CAI relationships obtained by UV laser-ablation MC-ICPMS. (For comparison, Leoville MRS3 is most like 144A in its isotope systematics, whereas Grosnaja 63624-1 is similar to E44). Weighted linear regression of the complete data set for 144A defines a $(^{26}Al/^{27}Al)_o$ value of 5.9 (±0.3 2σ) × 10^{-5}, with an intercept of 0.0 (±0.07 2σ) and an MSWD of 3.3 (Fig. 2 and table S1). An MSWD >1 indicates real variability in the data beyond analytical uncertainties. The isochron is dominated by melilites (with minor inclusions of spinel), because the melilite $Al_2Mg_{-1}Si_{-1}$ crystallographic substitution produces the greatest spread in Al/Mg in the CAI. Regression of the melilite data gives a line similar to the line defined by the combined data (and with the same MSWD). The data span up to the $(^{26}Al/^{27}Al)_o$ = 7 × 10^{-5} line defined by some bulk CAIs in this study and in (*10*). We conclude that inclusion 144A shows evidence for $(^{26}Al/^{27}Al)_o$ of at least 6 × 10^{-5} and probably higher.

Data for Efremovka E44 define a canonical value for $(^{26}Al/^{27}Al)_o$ (Fig. 3 and table S1). Results from this inclusion are relevant to the evidence for supra-canonical $(^{26}Al/^{27}Al)_o$ for two reasons: (i) this result (and similar results for Grosnaja 63624-1) shows that MC-ICPMS measurements reproduce the canonical value for $(^{26}Al/^{27}Al)_o$ that is so common among CAI anorthites; and (ii) the E44 data reveal the reason for the prevalence of the canonical $(^{26}Al/^{27}Al)_o$ values among CAIs and among anorthites in particular.

Results for all analyses of E44 define a line with a slope corresponding to $(^{26}Al/^{27}Al)_o$ = 4.8 (±0.3 2σ) × 10^{-5} and an intercept of 0.3 (±0.1 2σ) ‰ (Fig. 3). The MSWD for the E44 data combined is 2.3. Melilites from E44 taken by themselves define a different line corresponding to $(^{26}Al/^{27}Al)_o$ = 4.3 (±0.5 2σ) × 10^{-5}, with an intercept of 0.7 (±0.2 2σ) ‰ and an MSWD of 1.0 (Fig. 3). We interpret the unit MSWD of the melilites compared with the higher value for the combined data as an indication that melilites represent a single population (an MSWD of 1 indicates a single population), whereas the pooled data represent several populations marked by isotopic discordance.

The nonzero intercept for E44 melilites (Fig. 3) is a manifestation of a nonzero initial $\delta^{26}Mg^*$ and indicates exchange with a reservoir with higher $^{26}Mg^*/^{24}Mg$ and Al/Mg ratios. The only phase with higher Al/Mg and $^{26}Mg^*/^{24}Mg$ than melilite in E44 is anorthite, and addition of anorthite to the melilite regression leaves the latter unchanged; melilite and anorthite are on the same line. Similar relations involving melilite have been attributed to subsolidus closed-system isotopic exchange between anorthite and melilite (*13*). Closed-system exchange of Mg isotopes between these phases to the exclusion of others is expected because both minerals are characterized by relatively high rates of Mg self-diffusion (*14*, *15*).

Mg isotope exchange between melilite and anorthite has been seen in other CAIs, but the data for E44 are revealing because they show signs of exchange despite exhibiting a canonical $(^{26}Al/^{27}Al)_o$. Because the line defined by the melilite and anorthite data in E44 is probably the result of exchange of Mg isotopes between these phases, it follows that the anorthite complement of $^{26}Mg^*$ corresponding to the canonical $(^{26}Al/^{27}Al)_o$ is not representative of the initial value for the solar system. For the melilite $\delta^{26}Mg^*$ to define a nonzero intercept of 0.7 ‰ (Fig. 3), the anorthite with which it exchanged would have to have experienced a decrease in $\delta^{26}Mg^*$ of ~25 ‰ at some point during the history of the CAI. The alternative is that the melilite alone exchanged Mg isotopes with an outside reservoir enriched in $\delta^{26}Mg^*$ relative to its Al/Mg. Such an open-system exchange cannot be ruled out a priori, but it is difficult to explain why melilite would be susceptible to exchange, whereas anorthite was not given their comparably high Mg diffusivities (*14*, *15*). Open-system exchange also offers no explanation for the coincidence of the melilite and anorthite apparent isochrons.

Our data are consistent with a $(^{26}Al/^{27}Al)_o$ value of at least 6 × 10^{-5} and could be reconciled with the higher value of 7 × 10^{-5} recorded by some whole-rock CAIs (Fig. 1) if the Mg isotopes were disturbed as indicated by the MSWD >1 for Leoville 144A. In what follows, we use the conservative value of 6 × 10^{-5} defined by the best-fit isochron for 144A (Fig. 2).

Significance of supra-canonical $^{26}Al/^{27}Al$. Differences between supra-canonical and canonical $(^{26}Al/^{27}Al)_o$ values could be due to differences in time prescribed by the decay equation $(^{26}Al/^{27}Al)_t = (^{26}Al/^{27}Al)_o \exp(-\lambda \Delta t)$, where Δt is in years and $\lambda = 9.52 \times 10^{-7}$ $year^{-1}$, or they could result from differences in the Al isotope compositions of the reservoirs from which different CAIs formed. The nonzero initial $\delta^{26}Mg^*$ value for a CAI with canonical $(^{26}Al/^{27}Al)_o$ and the prevalence of the canonical $(^{26}Al/^{27}Al)_o$ value are most easily understood if the spread in $(^{26}Al/^{27}Al)_o$ has chronological importance. The indicated time interval Δt before final closure of the ^{26}Al-$^{26}Mg^*$ system based on the above expression, where $(^{26}Al/^{27}Al)_{(t)} = 4.5 \times 10^{-5}$ and $(^{26}Al/^{27}Al)_o$ = 6.0 × 10^{-5}, is 300,000 years. The widespread nature of the 4.5 × 10^{-5} value in feldspars (and in some other minerals) among CAIs supports the interpretation that these minerals record ^{26}Al-$^{26}Mg^*$ closure with a common solar-system-wide $(^{26}Al/^{27}Al)_o$. This closure must have followed nearly complete early resetting of the ^{26}Al-$^{26}Mg^*$ system. The alternative of different degrees of partial resetting for different objects would not result in a well-defined canonical value once ^{26}Al had decayed entirely to $^{26}Mg^*$.

The nonzero initial $\delta^{26}Mg^*$ of 0.7 (±0.2) ‰ for E44 melilite is consistent with exchange of Mg isotopes between melilite and feldspar for 300,000 (±100,000) years after initial growth

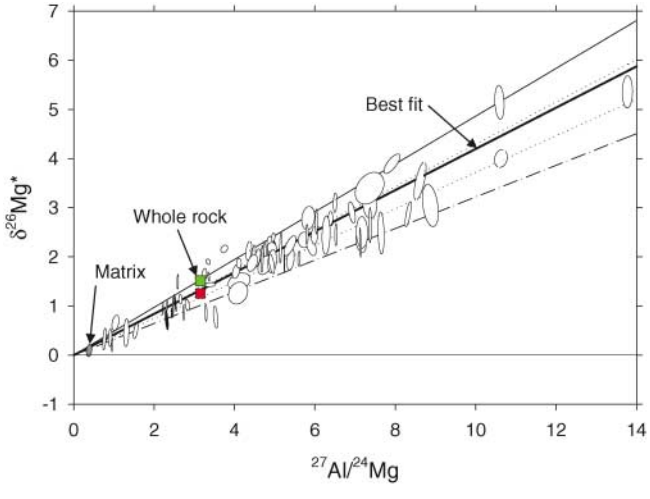

Fig. 2. Plot of $\delta^{26}Mg^*$ versus $^{27}Al/^{24}Mg$ values for CAI 144A (compact type A) from the Leoville CV3 meteorite obtained by laser-ablation MC-ICPMS. Each datum is shown as a 1σ error ellipse. Most data are above the canonical line (dash-dot line), and many are on or just below the 7 × 10^{-5} line (upper solid line) defined by some bulk CAI data. The data show a strong correlation with a best-fit slope corresponding to $(^{26}Al/^{27}Al)_o$ = 5.9 × 10^{-5} (heavy black line). Also shown is the whole-rock datum for 144A calculated for two different reference fractionation lines (green square and red square as in Fig. 1). The $(^{26}Al/^{27}Al)_o$ values of the reference lines are the same as in Fig. 1.

(Fig. 3), which supports the Δt of 300,000 years obtained from the spread in $(^{26}Al/^{27}Al)_o$ values. After 300,000 years of decay of ^{26}Al with $(^{26}Al/^{27}Al)_o = 6 \times 10^{-5}$, the $\delta^{26}Mg^*$ for the bulk $^{27}Al/^{24}Mg$ (volume-weighted average) composition of melilite and anorthite in E44 (the bulk $^{27}Al/^{24}Mg$ is ~6.5) would be 0.7 ‰. The values for 200,000 years and 400,000 years are 0.5 and 0.9 ‰, respectively, spanning the 0.2 ‰ uncertainty in the intercept. Because 0.7 ‰ is the value for the bulk composition consisting of melilite and anorthite in E44, complete isotopic equilibration between these minerals after 300,000 years would have resulted in both having an initial $\delta^{26}Mg^*$ of 0.7 ‰ (Fig. 3). Subsequent decay of ^{26}Al produces the observed melilite and anorthite data with a canonical $(^{26}Al/^{27}Al)_o$, reflecting the $^{26}Al/^{27}Al$ of 4.5×10^{-5} at Δt = 300,000 years, but with an initial $\delta^{26}Mg^*$ of 0.7 ‰ rather than 0 (Fig. 3) (*11*).

Thermal resetting of $^{26}Al/^{27}Al$ in CAIs. Our data constrain the thermal history of CAIs in the solar nebula. The constraints come from the rate of diffusion of Mg isotopes in melilite and anorthite (*14*, *15*) and the result that these minerals continued to exchange Mg isotopes until ~300,000 years after initial CAI growth (*11*). We constructed a model for diffusive homogenization of $^{26}Mg^*/^{24}Mg$ between anorthite and melilite for various volume fractions of the two minerals to assess the combinations of time and temperature required for resetting during a 300,000-year interval after initial CAI formation. In our calculations, we considered separately the effects of Mg isotope diffusion and $^{26}Mg^*$ accumulation due to ^{26}Al decay. Resetting after only 300,000 years (a time less than the mean life of ^{26}Al) ensures that these two processes occurred simultaneously. In this case, growth of $^{26}Mg^*$ in feldspar and melilite could have been punctuated by many episodes of diffusion during heating until final closure of the system after 300,000 years. The overall effect is the same as that portrayed in our calculation. Our model was calculated (*11*) for a concentration of $^{26}Mg^*$ in anorthite and melilite appropriate for 300,000 years of decay of ^{26}Al, with an initial $^{26}Al/^{27}Al$ of 6.0×10^{-5} and $^{27}Al/^{24}Mg$ values of 256 and 2.56 representing anorthite and melilite, respectively (yielding initial $\delta^{26}Mg^*$ values of 27.3 ‰ for anorthite and 0.3 ‰ for melilite before diffusive isotope exchange). Inclusion E44 has a radius of ~5 mm, so we used this size for the model.

The results are made universally applicable to the problem of melilite-anorthite Mg isotope exchange by presenting them in terms of the diffusion-reaction progress variable ξ (*16*). This progress variable is defined as:

$$\xi = \int_0^t \frac{D(T)}{z^2}\,dt \qquad (1)$$

where $D(T)$ is the temperature-dependent diffusion coefficient for Mg isotope exchange, z is the dimension of the diffusion medium, and t is time. Values for ξ show the combinations of the effective temperature (time-integrated temperature) and the time necessary to effect a specified amount of diffusive $^{26}Mg^*/^{24}Mg$ exchange between anorthite and melilite (Fig. 4).

The value of ξ required for complete homogenization of $\delta^{26}Mg^*$ between anorthite and melilite by Mg diffusion, where the difference between $\delta^{26}Mg^*$ in anorthite and melilite becomes 0, is 0.2 for the anorthite/(anorthite + melilite) = 0.25 volume fraction applicable to E44 (Fig. 4A). The attendant increase in melilite $\delta^{26}Mg^*$ of several tenths of a per mil due to the resetting is consistent with the observed excess in $\delta^{26}Mg^*$ in melilite at the model $^{27}Al/^{24}Mg$ (Fig. 3).

The resetting of the Mg isotopic system in melilite and anorthite requires 300 years at near-solidus temperatures of 1600 K (Fig. 4C). We adopt 1600 K as an absolute maximum subsolidus temperature for anorthite + melilite in CAIs but one that allows for partial melting of components near the eutectic (*17*, *18*). At 900 K, resetting takes 10^9 years. If conditions were suitable for resetting ^{26}Al-$^{26}Mg^*$ in E44 anorthite, they were more than sufficient to reset feldspars in most other CAIs (*19*) (Fig. 4) and probably in smaller Al-rich and Mg-poor grains of other minerals. CAIs with fewer, smaller anorthite grains would require lower ξ and, therefore, less time and temperature; other high-Al minerals of small size, perhaps with lower Mg diffusivities (e.g., hibonite grains), could also be reset under these conditions because the critical factor is ξ z^2 rather than $D(T)$ alone. For this reason the ξ for E44, an especially anorthite-rich CAI with unusually large grain size, represents a maximum for CAIs.

High temperatures that caused Mg diffusion like that evidenced in E44 must have occurred in the solar nebula. This is because the time scale for resetting the ^{26}Al-$^{26}Mg^*$ system at peak temperatures appropriate for asteroid-like parent bodies (~900 K) is 10^9 years and is inconsistent with parent-body thermal models, meteorite isotopic data, and geological evidence (*20*, *21*). This conclusion in no way detracts from the importance of later parent-body processes such as metamorphism and aqueous alteration that undoubtedly lead to further ^{26}Al-$^{26}Mg^*$ discordance in some CAIs.

Residence time of CAIs in the protoplanetary disk. The Δt of ~300,000 years indicated by our $(^{26}Al/^{27}Al)_o$ data is a reasonable estimate of the residence time τ for CAIs in the protoplanetary accretion disk of dust and gas that surrounded the sun. This is because Δt should also represent the time interval between initial CAI formation and the cessation of thermal processing and resetting of the ^{26}Al-$^{26}Mg^*$ chronometer; the residence time τ should be about equal to Δt. The resetting marked by Δt can be explained as the

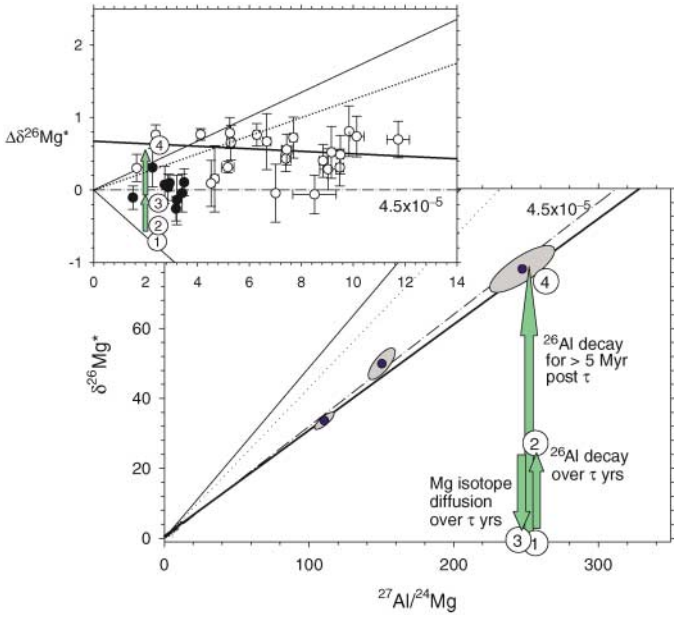

Fig. 3. Laser-ablation MC-ICPMS analyses of Efremovka CAI E44. Feldspars are shown as gray 1σ error ellipses in the lower panel, melilite and Al-Ti diopside as open and solid circles in the upper panel, respectively. The lower panel shows that a linear best fit for melilites and feldspars in E44 (heavy black line) is close to the canonical line (dash-dot line). The ordinate in the upper panel, $\Delta\delta^{26}Mg^* = \delta^{26}Mg^* - 0.32\ (^{27}Al/^{24}Mg)$, is the difference between $\delta^{26}Mg^*$ and the corresponding value for the canonical $(^{26}Al/^{27}Al)_o$ of 4.5×10^{-5} at the same $^{27}Al/^{24}Mg$. Error bars are 1σ. In this plot, the canonical evolution line is horizontal, and the absence of $^{26}Mg^*$ is shown by the lowermost negatively sloping solid line. The upper plot shows that melilites from E44 are above the canonical line and define an evolution line with a nonzero intercept of 0.7 ‰. All data for minerals other than feldspar for E44 appear in the lower left corner of the lower plot for reference. Also shown as numbered circles and arrows in the lower and upper panels is the evolution of feldspar and melilite, respectively. The minerals evolve by ^{26}Al decay and Mg isotope diffusive exchange in the first 300,000 years (the approximate residence time τ in the nebula) followed by uninterrupted ^{26}Al decay to reach their final compositions. The 7×10^{-5} and 6×10^{-5} reference lines from Fig. 1 are shown.

culmination of exposure to thousands of short-lived heating events for 10^5 years in the nebula.

The time that any solid particle of millimeter size spent en route to the sun from several astronomical units (AU) in the surrounding protoplanetary disk was likely to have been about 10^4 years (*22*). Because the radial velocity of the grains is proportional to circumstellar radius R, most of this time was spent inside of 3 AU in the protoplanetary disk (*22*), where high temperatures were most likely. One site where high temperatures prevailed was near the growing sun ($R \sim 0.06$ AU) (*23*). Temperatures approaching and/or exceeding the melting point of CAIs have been postulated for the "reconnection ring" region of the gap between the accretion disk and the nascent sun (*23*, *24*). Here, proto-CAIs were exposed to flares and ambient temperatures that heated them to temperatures of about ≤1700 K (*24*). The residence time of a CAI in this region is believed to have been approximately 10 to 20 years (*24*). With a residence time in the ring of 20 years and a total high-temperature exposure time of ~300 years [from the diffusion progress ξ at 1600 K (Fig. 4)], CAIs like E44 would have had to enter the zone of heating about 15 times during their lifetimes in the nebula to reset the ^{26}Al-^{26}Mg* melilite-anorthite system. The multiple trips to the hot zone can be explained by entrainment of the CAIs in magneto-centrifugally driven x-winds emanating from the inner edge of the disk. In this way, the CAIs are launched back out to the more distal regions of the disk. The transport of material back to the disk by this process is considerably faster than inward drift rates through the disk (*24*). Although unlikely, if each trip from $R \geq 3$ AU to the reconnection ring took about 3×10^4 years (*22*), the total time required is about 4.5×10^5 years [15 trips × (3×10^4) years per trip]. The combination of ξ for Mg isotope diffusion and estimated transport times therefore indicates a nebular τ of 10^5 years for CAIs.

Another means of imparting high temperatures to CAIs is by passage through shock waves in the disk. Shock heating has been used to explain the cooling histories of chondrules, for example. Models for the process of shock heating in the nebula suggest that millimeter objects passing through the high-density waves experience temperatures of 1400 K to 2200 K for up to one day (*25*). Such events would have disturbed the ^{26}Al-^{26}Mg* system in CAIs after their formation.

Wood (*26*) proposed that spiral density waves in the nebula could be the shock waves responsible for heating rock materials. He described a circumstance in which two waves symmetrically distributed in the nebula travel with orbital periods on the order of 900 years, independent of circumstellar distance R. For material in quasi-Keplerian orbit in the inner solar nebula, these waves would have behaved as if they were effectively stationary. In this situation, the total time required to achieve resetting of the ^{26}Al-^{26}Mg* system in anorthite and melilite (300 years at 1600 K for ξ = 0.2) by passage of CAIs through the shocks is

$$\tau = (1/R)\int_0^R \Omega^{-1} d\mathrm{R}(N/2) \qquad (2)$$

where Ω is the Keplerian angular velocity $[R/(1\ \mathrm{AU})]^{-3/2}$ and N is the number of 1-day shock episodes required to achieve the requisite value for ξ. In this case, N must add up to 300 years of heating, which requires that $N = 300 \times 365 = 109{,}500$ 1-day shocks. The τ obtained from this scenario for a CAI drifting inward from about 3 AU is 2.3×10^5 years. The precise value for τ is sensitive to the exact time-integrated temperature of processing, but for reasonable effective shock temperatures of ≥ ~1500 K, the indicated nebular residence time τ is on the order of 10^5 years (the value for τ using 1500 K is 8×10^5 years). Melting of a CAI at higher temperatures would also reset the ^{26}Al-^{26}Mg* chronometer by rapid diffusion but can not explain the data for E44.

In both scenarios for high-temperature processing, we obtain a τ of 10^5 years. The derived τ explains the resetting of $(^{26}\mathrm{Al}/^{27}\mathrm{Al})_o$ in some CAIs from $\geq 6 \times 10^{-5}$ to 4.5×10^{-5} and the nonzero initial δ^{26}Mg* in E44 and in many other CAIs (*13*, *27*). Combining this result with the 10^4 years required for inward drift from 3 AU or beyond (*22*) suggests that CAIs like those examined here made several passes through the inner protoplanetary disk.

The meaning of the canonical $(^{26}\mathrm{Al}/^{27}\mathrm{Al})_o$ as a reflection of τ should apply to most CAIs, because conditions suitable for resetting ^{26}Al-^{26}Mg* in E44 anorthite in the first 10^5 years are more than sufficient to reset most feldspars and probably other, smaller Al-rich Mg-poor minerals typical of CAIs. Accordingly, Mg isotope resetting in CAIs with similar τ should record the same "canonical" $(^{26}\mathrm{Al}/^{27}\mathrm{Al})_o$, because it arises from uninterrupted ^{26}Al decay for $t > \tau$. Where $(^{26}\mathrm{Al}/^{27}\mathrm{Al})_o$ is less than canonical, Al isotope heterogeneity

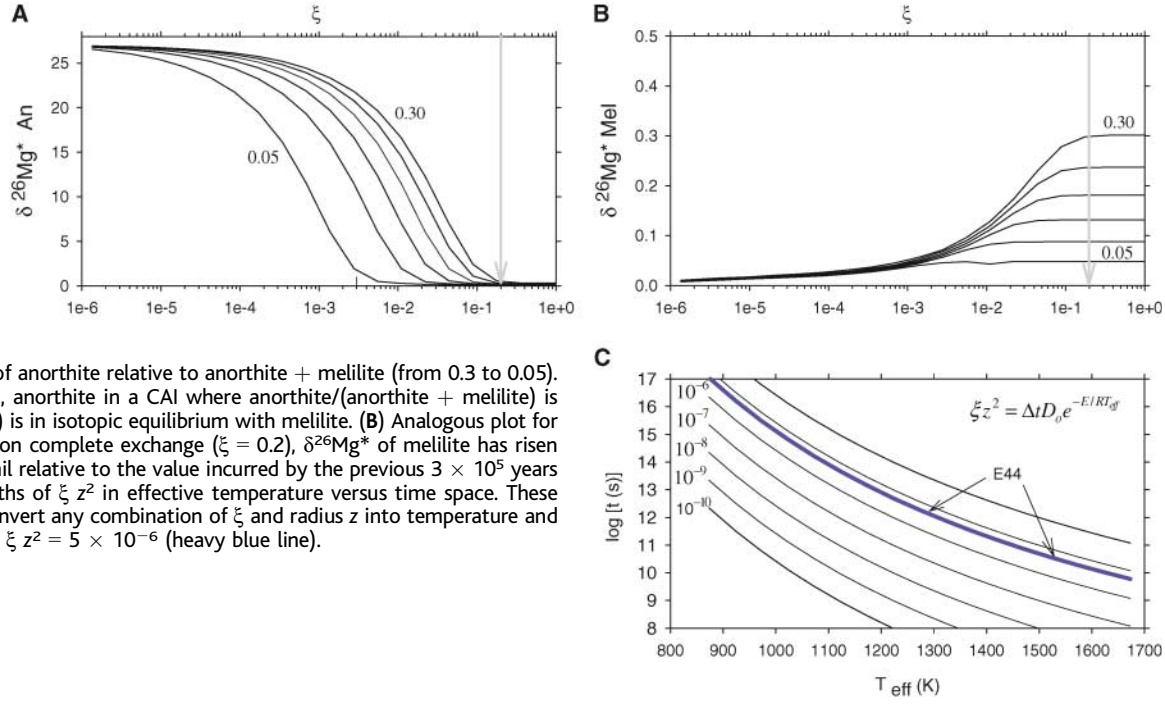

Fig. 4. Results of diffusion calculations expressed in terms of the diffusion-reaction progress variable ξ for a 10-mm diameter CAI (i.e., the size of E44). The initial condition corresponds to 3×10^5 years of ^{26}Al decay. (**A**) The reduction in δ^{26}Mg* in anorthite as measured relative to the initial melilite value. Isopleths are for different volume fractions of anorthite relative to anorthite + melilite (from 0.3 to 0.05). At ξ = 0.2 (gray arrows), anorthite in a CAI where anorthite/(anorthite + melilite) is 0.25 by volume (i.e., E44) is in isotopic equilibrium with melilite. (**B**) Analogous plot for melilite showing that upon complete exchange (ξ = 0.2), δ^{26}Mg* of melilite has risen several tenths of a per mil relative to the value incurred by the previous 3×10^5 years of ^{26}Al decay. (**C**) Isopleths of ξ z^2 in effective temperature versus time space. These curves can be used to convert any combination of ξ and radius z into temperature and time. In the case of E44, ξ $z^2 = 5 \times 10^{-6}$ (heavy blue line).

or subsequent (possibly parent body) processing is indicated.

References and Notes

1. H. C. Urey, *Proc. Natl. Acad. Sci. U.S.A.* **41**, 127 (1955).
2. M. Wadhwa, S. S. Russell, in *Protostars and Planets IV*, V. Mannings *et al.*, Eds. (University of Arizona Press, Tucson, AZ, 2000), pp. 995–1018.
3. T. Lee, D. A. Papanastassiou, *Geophys. Res. Lett.* **1**, 225 (1974).
4. Y. Amelin, A. N. Krot, I. D. Hutcheon, A. A. Ulyanov, *Science* **297**, 1678 (2002).
5. G. J. MacPherson, A. M. Davis, E. K. Zinner, *Meteoritics* **30**, 365 (1995).
6. S. S. Russell, G. Srinivasan, G. R. Huss, G. J. Wasserburg, G. J. MacPherson, *Science* **273**, 757 (1996).
7. M. Bizzarro, J. A. Baker, H. Haack, *Nature* **431**, 275 (2004).
8. A. Galy, E. D. Young, R. D. Ash, R. K. O'Nions, *Science* **290**, 1751 (2000).
9. E. D. Young, R. D. Ash, A. Galy, N. S. Belshaw, *Geochim. Cosmochim. Acta* **66**, 683 (2002).
10. A. Galy, I. D. Hutcheon, J. N. Grossman, Lunar and Planetary Science Conference XXXV, 15 to 19 March 2004, Houston (Lunar and Planetary Institute, Houston, TX, 2004).
11. Materials and methods are available as supporting materials on *Science* Online.
12. K. I. Mahon, *Int. Geol. Rev.* **38**, 293 (1996).
13. F. A. Podosek *et al.*, *Geochim. Cosmochim. Acta* **55**, 1083 (1991).
14. T. LaTourrette, I. D. Hutcheon, Lunar and Planetary Science Conference XXX, 15 to 19 March 1999, Houston (Lunar and Planetary Institute, Houston, TX, 1999).
15. T. LaTourrette, G. J. Wasserburg, *Earth Planet. Sci. Lett.* **158**, 91 (1998).
16. O. Lovera, F. M. Richter, M. H. Harrison, *J. Geophys. Res.* **94**, 17017 (1989).
17. J. P. Greenwood, Lunar and Planetary Science Conference XXXV, 15 to 19 March 2004, Houston (Lunar and Planetary Institute, Houston, TX, 2004).
18. E. M. Stolper, *Geochim. Cosmochim. Acta* **46**, 2159 (1982).
19. For example, in a CAI the same size as E44 but with anorthite/(anorthite + melilite) = 0.05 rather than 0.25, the anorthite + melilite system would be reset when reaction progress variable = 0.4×10^{-3}, corresponding to 10 years at 1600 K or 10^7 years at 900 K.
20. H. Y. McSween, A. Ghosh, R. E. Grimm, L. Wilson, E. D. Young, in *Asteroids III*, W. Bottke *et al.*, Eds. (University of Arizona, Tucson, AZ, 2003), pp. 559–571.
21. K. Keil, *Planet. Space Sci.* **48**, 887 (2000).
22. S. J. Weidenschilling, *Icarus* **165**, 438 (2003).
23. F. H. Shu, H. Shang, T. Lee, *Science* **271**, 1545 (1996).
24. F. H. Shu, H. Shang, M. Gounelle, A. F. Glassgold, T. Lee, *Astrophys. J.* **548**, 1029 (2001).
25. S. J. Desch, H. C. Connolly, *Meteorit. Planet. Sci.* **37**, 183 (2002).
26. J. A. Wood, *Meteorit. Planet. Sci.* **31**, 641 (1996).
27. G. J. MacPherson, A. M. Davis, *Geochim. Cosmochim. Acta* **57**, 231 (1993).

28. The authors wish to thank A. Krot for providing sample E44. The work was supported by grants from the NASA Cosmochemistry program, the NASA Astrobiology Institute, the Particle Physics and Astronomy Research Council (UK), and the National Science Foundation (USA).

Supporting Online Material

www.sciencemag.org/cgi/content/full/1108140/DC1
Materials and Methods
SOM Text
Figs. S1 to S8
Table S1
References

1 December 2004; accepted 11 February 2005
Published online 3 March 2005;
10.1126/science.1108140
Include this information when citing this paper.

Structure of a γδ T Cell Receptor in Complex with the Nonclassical MHC T22

Erin J. Adams,[1,2,3] Yueh-Hsiu Chien,[1,3] K. Christopher Garcia[1,2,3]*

γδ T cell receptors (TCRs), αβ TCRs, and antibodies are the three lineages of somatically recombined antigen receptors. The structural basis for ligand recognition is well defined for αβ TCR and antibodies but is lacking for γδ TCRs. We present the 3.4 Å structure of the murine γδ TCR G8 bound to its major histocompatibility complex (MHC) class Ib ligand, T22. G8 predominantly uses germline-encoded residues of its δ chain complementarity-determining region 3 (CDR3) loop to bind T22 in an orientation substantially different from that seen in αβ TCR/peptide-MHC. That junctionally encoded G8 residues play an ancillary role in binding suggests a fusion of innate and adaptive recognition strategies.

γδ T cells, like αβ T cells and B cells, generate a diverse repertoire of antigen-recognition receptors through somatic rearrangement of V, D, and J gene segments. This process generates a heterodimeric receptor composed of two chains, each encoding a variable (V) and constant (C) domain. It has been convincingly demonstrated that αβ and γδ T cells have different functional roles in the immune system (*1*), yet the identity of endogenous ligands for γδ T cells is unclear and little is known about the molecular basis of ligand recognition through their specific γδ TCRs. From the few defined γδ TCR ligands, it is apparent that γδ TCRs recognize a diverse array of antigens and that, like antibodies, they appear to recognize these antigens directly, distinguishing them from αβ TCRs that require antigen presentation by MHC [reviewed in (*2*)].

Early immunogenetic studies of αβ TCR and antibodies gave strong clues into the structural properties by which they would recognize ligand (*3*). In αβ TCR there is a concentration of diversity in the CDR3 (10^{15} unique junctions), relative to germline-encoded CDR1 and CDR2 derived from V-domain pairing (2500 pairs). In contrast, antibodies exhibit less CDR3 junctional diversity (10^{11} unique junctions) relative to the germline-encoded diversity of their CDR1 and CDR2 loops (90,000 pairs). Consistent with this, structural studies showed that the αβ TCR CDR3 primarily contact antigenic peptide, while CDR1 and CDR2 loops contact conserved helical portions of the MHC surface (*4*). Antibodies, although predominantly using CDR3, also make substantial use of CDR1 and CDR2 in recognizing a diverse antigenic repertoire.

A similar analysis of the γδ TCR repertoire indicates that they have the highest potential CDR3 diversity (10^{18}) but limited diversity conferred by pairing of germline-encoded V domains, with only ~7 Vγs and ~10 Vδs in the mouse (70 potential pairs) (*3*, *5*). CDR3 length distribution in γδ TCRs is more similar to antibodies than to αβ TCRs in that the CDR3δ loops are long and variable, and the CDR3γ loops are short and constrained (*5*). Given the long and potentially diverse CDR3δ of γδ TCR, it would seem likely that this loop is used directly for antigen recognition. However, many infection models involving γδ T cells show restricted V-gene usage (*6*), which suggests that γδ TCR specificity is determined by germline-derived V domains alone.

We have determined a 3.4 Å crystal structure of the γδ TCR G8 in complex with the nonclassical MHC Ib protein T22 (*7*, *8*). The G8 γδ heterodimer binds protein products of the T22 and T10 loci (95% homology), as do 0.09 to 0.6% of γδ T cells in the spleen and intraepithelial lymphocytes (IELs) of unstimulated mice (*9*, *10*). Both T22 and T10 have a canonical class I fold, except that the C terminus of the α2 helix is unraveled, disrupting the peptide-binding groove and exposing the underlying β-sheet platform (*11*, *12*). Binding measurements with refolded T22 (*9*) and the lack of a bound ligand in the structures of T10 (*12*) and T22 (*11*) confirm that G8 recognition of T10/T22 is direct and not dependent on antigen processing. The structure shows that the CDR loops, predominantly germline-encoded residues of the junctionally recombined CDR3δ, are directly used in γδ TCR recognition of an MHC ligand, resulting in a binding mode distinct from either antibody/antigen or αβ TCR/pMHC interactions.

Expression and structure determination of the γδ TCR and its ligand. The soluble G8 γδ TCR and its MHC ligand, T22, were expressed from baculovirus-infected insect cells, which produced a glycosylated G8 γδ TCR containing the canonical interchain di-

[1]Department of Microbiology and Immunology, [2]Department of Structural Biology, [3]Program in Immunology, Stanford University School of Medicine, Fairchild D319, 299 Campus Drive, Stanford, CA 94035–5124, USA.

*To whom correspondence should be addressed. E-mail: kcgarcia@stanford.edu